



Thermal modeling, exergy analysis, performance of BIPV and BIPVT: A review



Mary Debbarma^a, K. Sudhakar^{a,b,*}, Prashant Baredar^a

^a Energy Centre, Maulana Azad National Institute of Technology Bhopal, India

^b Faculty of Mechanical Engineering, Universiti Malaysia Pahang, 26600 Pahang, Malaysia

ARTICLE INFO

Keywords:

Photovoltaic
BIPV
BIPVT
Thermal modeling
Simulation software
Comparison

ABSTRACT

People are becoming more and more sensitive to the ecological consequences of global warming and environmental devastation. The objective is to replace the use of fossil fuel energy with renewable forms of energy. In the field of building construction, this leads to a new legislation frameworks and radical changes in how we design our buildings. The use of renewable in the building envelope is much varied and opens many opportunities for creative designers. Many architects have already integrated PV successfully in their buildings. This paper reviews the present day application of BIPV and BIPV-T technologies. In addition to it thermal modeling, energy and exergy analysis of BIPV and BIPVT system are also discussed. This study also reviews the recent developments of the technology worldwide.

1. Introduction

Several strategies have been adopted to resolve the issues related to global warming, CO₂ emissions, depleting fossil fuel reserves which are gaining serious concern in the current global energy scenario. The existing renewable technologies which are based on solar energy are considered the most promising for saving energy and reducing carbon emissions. Among all the renewable sources the most abundant energy source available is solar energy which is found both in direct as well as indirect forms [1]. The solar energy can suitably be used for Solar Thermal Collectors (STC) and Photo Voltaic (PV) panels, which today are the most practical options for building applications [2]. Sustainable solar technologies like PV and STC provide greater opportunity for integration into the building roof or wall structure [3].

The photo thermal conversion technology is an important application of solar energy for daily life, such as domestic hot water, drying etc. Through the energy transformation of light–heat–electricity the photo thermal conversion technology is also used to satisfy the electric energy requirement. The photo thermal conversion technology also collects the solar energy by using large-scale parabolic mirror arrays, which further convert it to the thermal energy of working medium [4].

Solar photovoltaic technology is one of the simplest methods of

converting solar energy into electricity which uses the principle of semiconductor. It is a direct conversion of sunlight into electricity without using any interface. Solar PV systems are simple in design, modular in the nature, rugged, requires a little maintenance and stand alone can generate the power from microwatts to megawatts [5]. The key component of the photovoltaic technology is the photovoltaic module formed of one or more solar cells first connected in series and then packed. The photovoltaic technology is not restricted by region since the solar energy that reaches the earth is spread out over a vast area. Moreover, photovoltaic is a reliable, pollution-free safe and noiseless technology. Over recent years the photovoltaic technology has obtained significant development, especially in building integrated photovoltaic (BIPV) and building integrated photovoltaic thermal (BIPVT) hybrid system. Research on building-integrated photovoltaic is also increasing day by day. For obtaining specific building designs many efforts are given at the design level [6].

The objectives of this study are as follows:

- To review the analytical expressions used for thermal modeling and exergy analysis of the BIPV, BIPVT air and water collector.
- To identify the suitable simulation software's for BIPV and BIPV-T systems.

Abbreviations: CdTe, Cadmium Telluride; CIS, Copper Indium Gallium Selenide; GaAs, Gallium Arsenide; DC, Direct current; NZEB, Net-zero energy buildings; BIPV, Building-integrated photovoltaic; BAPV, Building applied photovoltaic; BIPVT, Building-integrated photovoltaic with thermal; PV, Photo-voltaic; c-Si, Crystalline silicon; a-Si, Amorphous Silicon; m-Si, Multicrystalline Silicon; p-Si, Polycrystalline Silicon; HIT, Heterojunction Intrinsic Thin layer; EFG, Edge defined film fed growth; PE-CVD, Plasma-enhanced chemical vapor deposition; PEC, Photo electrochemical Cells; STC, Standard Testing Condition; CAD, Computer aided designing; MPPT, Maximum power point tracker; NOCT, Nominal Operating Cell Temperature; PCM, Phase Change Material; ETFE, Ethylene tetrafluoroethylene

* Corresponding author at: Energy Centre, Maulana Azad National Institute of Technology Bhopal, India.

E-mail address: sudhakar.i@manit.ac.in (K. Sudhakar).

<http://dx.doi.org/10.1016/j.rser.2017.02.035>

Received 6 August 2015; Received in revised form 24 January 2017; Accepted 6 February 2017

1364-0321/© 2017 Elsevier Ltd. All rights reserved.

Nomenclature			
<i>Subscript</i>		T_{amb}	Ambient temperature
T_{sky}	Sky temperature	\dot{Q}	Convective and radiative heat transfer coefficient from photovoltaic cell to ambient
T_{out}	Outside ambient temperature	$E_{x,solar}$	Exergy rate from the solar irradiance
G	Solar radiation	Ex_{in}	Input exergy (radiation exergy)
h_i	Interior heat transfer coefficient	Ex_o	Output exergy
T_{airout}	Outlet air temperature	Ex_{th}	Thermal exergy
U_{bb}	overall heat transfer for insulation plate	Ex_{PVT}	Photovoltaic thermal exergy
U_{tair}	overall heat transfer for duct	A_c	Collector area
T_r	Room air temperature	N	Number of covers or glazing layers
F_R	Heat removal factor	N_c	Number of collectors
C_p	Specific heat of the collector cooling medium	h_w	Convection heat transfer due to the wind.
F	Fin efficiency	S	Solar radiation
F'	Corrected Fin efficiency	T_s	Sun temperature ($T_s = 5777$ K)
M	Thermal conductivity of the absorber	Ex_d	Exergy destruction or irreversibility
U_{loss}	Overall heat loss coefficient of the collector	S_{gen}	Entropy generation rate
p	Collector perimeter	IP	Improvement potential
t	Absorber thickness	<i>Greek Letters</i>	
T_{pm}	Mean collector plate temperature	β	Collector mounting
h_w	Forced convection heat transfer coefficient	σ	Stefan-Boltzmann constant
v	wind velocity	ϵ_g	Emittance of the cover or glazing
h_{nat}	Natural convection loss	ϵ_p	Emittance of the plate
T_a	Ambient temperature	ϵ_p	Plate emissivity
U_{top}	Overall top loss heat transfer coefficient	$\tau\alpha_T$	Transmittance-absorptance product of the collector material
Gr	Grashof number	ψ	Exergy efficiency
\dot{E}_x	Exergy of the BIPV		
T_{mod}	Module Temperature		

– To compare the thermal performance of new design of BIPV and BIPVT system worldwide.

2. PV technologies for building integration

Using PV technology building integrated photovoltaic system (BIPV) and building integrated photovoltaic thermal hybrid system (BIPVT) can be considered as energy efficient system as well as energy production like weatherproofing, insulation, and even structural strength to the building [7].

The leading technology in the field of BIPV and BIPVT is the Photovoltaic (PV). In extreme hot climatic conditions the efficiency of the PV module can be regained by minimizing the temperature of the module. Thus electricity and heat can be produced from the solar energy through BIPVT system (Fig. 1).

Based on thickness, types of material, types of junction and generation, PV technologies can be classified as:

2.1. Crystalline technology

Crystalline silicon (c-Si) is chosen as the first choice for solar cell as it forms the base for the semiconductor technology. Its efficiency is up to 20%. Its main advantage is that it is the second most abundant material on the earth. The brief overviews of crystalline materials are:

2.1.1. Mono-crystalline silicon

In order to produce mono-crystalline silicon cells high purity single crystal Si rods are prepared and then sliced them into thin wafers. To manufacture the monocrystalline silicon crystalline Si p-n junctions are used which are generally cut from cylindrical ingots from which a single crystal ingot is cultivated further using the Czochralski method. The efficiency of mono-crystalline silicon cells is between 17–18% because of its purity. Because of its high efficiency it is worldwide in a large scale [9].

2.1.2. Poly-crystalline silicon

Poly-crystalline cell manufacturing is started by melting silicon and solidifying it into orient crystals in a fixed direction producing rectangular ingot of multi-crystalline silicon which are sliced into blocks and finally into thin wafers. However, this final step can be replaced by cultivating wafer thin ribbons of poly-crystalline silicon. For reducing the cost for developing PV module, poly-crystalline silicon cell is the best suitable material and its cost is low compared to the mono-crystalline silicon cell. Poly-crystalline silicon cell are made from sawing a cast block of silicon first into bars and then wafers. The efficiency of poly-crystalline silicon is in between 13–14% [10–13].

2.1.3. Ribbon cast silicon

Ribbon cast Silicon are of two types: Edge defined film fed growth (EFG) and String ribbon.

Edge defined film fed growth (EFG) is a novel crystal growth

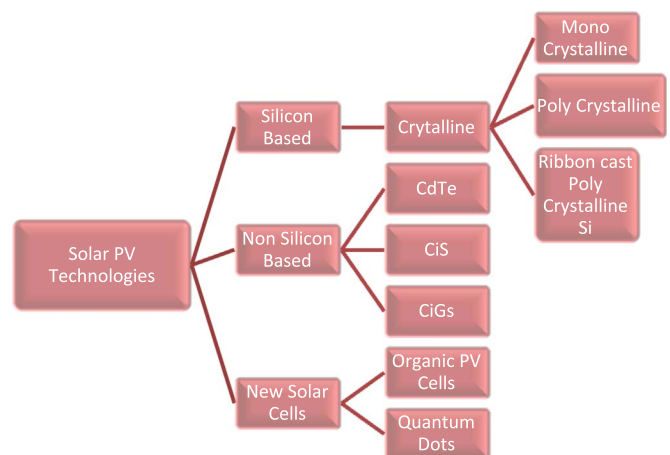


Fig. 1. Brief view of PV technologies [8].

technique widely used for the growth of sapphire, silicon and LiNbO_3 and other materials in different shapes like plates, tubes and rods [14].

String Ribbon Si wafers is manufactured with the help of a vertical sheet growth technique. In this process a low cost Si is produced because Si feedstock is used and ingot sawing and wafer etching are absent. Because of this reason cost of wafer production of ribbon wafers are low compared to others which are obtained from directionally solidified and cast ingots or CZ boules. Defects in ribbon silicon are: they are dependent on thermal history, metal precipitation are influenced by fast crystallization \rightarrow small precipitates. Gettering and hydrogenation differs from ingot mc-si which is more effective [15].

2.2. Thin film solar cells

In thin film technology, a very thin layer of semiconductor material ranging from nanometer level to several micrometer in thickness is deposited on the either coated glass or stainless steel or a polymer substrate. Thin film technology is very cheap and economic as compared to the crystalline silicon solar cells because of its low manufacturing cost and lesser usage of materials. To reduce the amount of light-absorbing materials required to construct the solar cell various thin film technology are being developed. This result in reduction of processing cost and conversion efficiency compared to crystalline silicon cells which is about 7–10%. Larger land and longer collector area are required for thin film technology since their efficiency are very less for same energy requirement. These are used where nonproductive land is available such as Rajasthan [8–10].

2.2.1. Amorphous silicon

Amorphous silicon has no fixed crystal structure. Many covalent bands are incomplete due to randomness of atoms. Conversion efficiency of amorphous silicon ranges between (4.5–8.5)% which is higher as compared to wafer/ribbon-based silicon modules. Silicon film cell are deposited by chemical vapor deposition mainly plasma-enhanced PE-CVD process from saline gas and hydrogen gas. Depending on the deposition parameter it can be amorphous silicon, polycrystalline silicon, nanocrystalline silicon. A-Si is a substitute to single or multi-crystalline cells. The main disadvantage of this cell is its low efficiency which is about 4% [9].

2.2.2. Cadmium telluride (CdTe)

CdTe is based on Cadmium telluride which is an efficient light absorbing material for thin film cells. CdTe has a direct band gap of 1.44 eV. With n-type CdS and p-type CdTe thin film heterogeneous junction is fabricated. Its efficiency is about 15%. Solemn carried out an experiment to enhance the characteristic of solar cell which shows the chemical heat treatment is required to produce better cells [13].

2.2.3. Copper indium gallium selenide

Since it is a new technology this material is still in development phase and is set to compare with other silicon solar cell. Its efficiency is about 21%. CIS has a direct band gap of 1.0 eV. A heterogeneous junction of Ga into the CIS mixture increases the band gap beyond 1.1 eV. Main advantage of this technology is its preparation is not so expensive and it is more stable as compared to a Si cell in outdoor applications. It is also known for its stability for longer time [13].

2.2.4. Cu_2S solar Cells

Cu_2S is one of the simplest solar cells to be produced which is produced using simple conversion technique. The highest efficiency acquired is almost 10%. Due to the emergence of higher efficiency Si cells, this cell lost the battle of survival. Stability of these cells due to cuprous-cupric conversion technique is a concern [12].

2.3. Concentrating solar cells

2.3.1. Gallium arsenide (GaAs)

GaAs is known to be a lucrative PV material having a direct band gap of 1.43 eV. It is a compound semiconductor formed by gallium and arsenic that has almost a similar structure with silicon. Its efficiency can be increased by alloying it with certain materials such as Al, P and Sb which will form multi junction devices. On the other hand band gap values will also be improved. But the production cost of GaAs is very high due to its usage in extraterrestrial and several other applications [13].

2.4. Hybrid solar cell

Hybrid means combining of two or more things in a single system. In hybrid solar cell crystalline silicon cell is generally combined with non-crystalline silicon. Organic and inorganic semiconductors are incorporated in this cell. It have organic materials that consist of conjugated polymers that absorb light as the donor and transport holes in an organic material which is mixed with a high electron transport material to form the photoactive layer and two materials are assembled together in a hetero junction type photoactive layer, which have a greater power conversion efficiency than a single material. Among these two material one acts as donor and the other as photon absorber. Efficiency of this cell is better than the other cells [8–10].

2.5. Organic solar cell

It is a new and low cost latest technology. Recently the power conversion efficiency of the organic cell is found to be about more than 9% but further enhancement of 10% is required for commercial purposes. Currently it is in developing phase and mostly focused towards developing high efficiency and stable devices with both conventional and inverted solar cell configuration based on donor according to organic and hybrid solar cell group. Thin films (typically 100 nm) of organic semiconductors such as polymers and small-molecule compounds like carbon fullerenes, polyphenylene vinylene, pentacene and copper phthalocyanine (a blue or green organic pigment). At present with the help of conductive polymers the maximum efficiency achieved is (4–5) %; however, the main attraction in this material exists in its mechanical flexibility and disposability [13].

2.6. Dye- sensitized solar cell

It is a very new technology developed. Due to the many problem faced by other solar cell such as efficiency, production cost, design, and some environmental problems researchers have come with a new idea of producing dye-sensitized solar cell.

The very first persons to discover dye sensitized solar cell are by Michael Gretel and Dr Brian Oregano in the year of 1991. It is based on a semiconductor formed between a photosensitized anode and an electrolyte (a photo electrochemical system). It has many advantages compared to other solar cell like high efficiency, environmentally more suitable, low cost, easy manufacturing process, semi flexible and most of all material used are cheap [8–10].

2.7. New & emerging excitonic cells

Some new and emerging excitonic cells are listed below:

- i) Photo electrochemical (PEC) Cells: Efficiency is about 12%.
- ii) Organic Plastic Cells: Polymer/polymer, Polymer/inorganic semiconductor junction: Efficiency is up to 9%.
- iii) Multijunction and Carbon Nanotube based solar Cells [14–18] (Table 1).

Table 1
Values of Module efficiency and temperature coefficient for different PV modules: [5,16–19].

Type of PV module	Module Efficiency at STC (%)
a-Si	12.2 ± 0.3
m-Si	18.5 ± 0.4
p-Si	22.4 ± 0.6
CdTe	17.5 ± 0.7
CIGS	15.7 ± 0.5
HIT	17.00
GaAs	24.1 ± 1.0
Organic	8.7 ± 0.3 m

Building-integrated photovoltaics (BIPV) are the method of incorporating the PV module into a new building as a source of electrical power though they can also be retrofitted in the existing buildings. BIPV can act as a standard building envelope material and supply electricity at the same time. It can add to aesthetics compared to other conventional faced or roof mounted photovoltaics (PV). But, it is adopted very less as its market share in all PV installations is in the order of (1–3) % worldwide [20]. There are two principal categories of mounting building photovoltaic array systems: BIPV and BAPV.

BIPV is the method of integrating various types of PV modules architecturally in a new building structure and the conventional roofing materials, such as shingles, tiles, slate and metal roofing can be replaced [21].

BAPV is an add-on to the existing building, which is indirectly related to the structure’s functional aspects. The major classification for BAPV systems are Rack-mounted arrays and Standoff arrays. Rack-mounted arrays are introduced on flat roofs in such a way that the modules are at an optimum orientation and tilt for the application. Standoff arrays are generally mounted above the roof surface and parallel to the slope of a pitched roof [21] (Figs. 2 and 3).

The biggest obstacle in the larger adoption of BIPV modules is its cost which is higher as compared to standard PV modules. This problem can be overcome by lowering the installation cost and traditional building envelope material. BIPV can be grouped into two main categories: roofing systems and façade systems. Roofing systems include skylights, standing seam products, tiles and shingles. Façade systems include glazing, spandrel panels, and curtain wall products [21] (Table 2).

BIPVT system represents the combination of standard thermal collectors and PV panel that are integrated into the building. These systems are capable of producing electrical and thermal energy for the building. [2] BIPVT products are considered as a replacement material for traditional roofing or façade cladding. BIPVT system produces more energy than the BIPV system using the same façade or roof area [20] (Fig. 4).

BIPVT system can be integrated in various ways as thermal cooling medium, ducts, phase change materials, water collector integrated into the roof (Table 3).

3. Modeling and simulation of BIPV and BIPVT system

A simulation is basically done to study the feasibility of a system in favorable climatic conditions like temperature, humidity before doing it practically. Various parameters are tested in suitable simulation software and the model accuracy is tested by changing the data [12]. The experimental results of model can be compared with the results of analytical models; both with reference situations and with experimental measures obtained in real-site test facilities (in different climatic conditions [12].

The literature review reveals that:

- 1) Most of the energetic simulations are related to BIPV systems.

- 2) Thermal simulations of BI solar systems are mostly about BIPVT.
- 3) Some studies combine energetic and thermal simulation (most of these investigations are about BIPVT) (Table 4).

4. Thermal modeling

4.1. Thermal modeling of BIPV

4.1.1. Heat transfer across the PV panel

The energy balance equation of a PV panel layer is shown in Eq. (1), where T_{out} - outside ambient temperature.

G -solar radiation.

T_{sky} - sky temperature.

h_c - convective heat transfer coefficient for exterior [48,49].

$$-\frac{(T_{epv} - T_{mpv})}{\frac{R_{pv}}{2}} - \epsilon_{pv} \sigma (T_{epv}^4 - T_{sky}^4) - h_c (T_{epv} - T_{out}) = 0 \tag{1}$$

$$M_{pv} \cdot C_{p_{pv}} \cdot \frac{dT_{mpv}}{dt} = \alpha_{pv} \cdot G + \frac{(T_{epv} - T_{mpv})}{\frac{R_{pv}}{2}} - \frac{(T_{mpv} - T_{ipv})}{\frac{R_{pv}}{2}} \tag{2}$$

4.1.2. Heat transfer within air gap

The heat transfer in the air gap is governed by natural convection although the radiation effects are considered assuming a view factor (FR_{pv-pcm}) of 1 between planes [50]. The convective heat transfer coefficients inside air cavity are influenced by the operation mode of the system (open or closed vents) [51].

For closed vents: Heat transfer coefficients are based on the Kalogirou [50] correlation.

For open vents: The convective heat transfer coefficient is based on Duffie and Beckman [49] correlation.

The mean air velocity in gap is obtained by solving Bernoulli’s equation and assuming linear variation for air density and temperature as described in Kalogirou [50].

The energy balance within the air gap is described by the following equations:

$$\frac{(T_{mpv} - T_{ipv})}{\frac{R_{pv}}{2}} - h_{pvac} (T_{ipv} - T_{ac}) - h_r (T_{ipv}^4 - T_{ew}^4) = 0 \tag{3}$$

$$M_{air} \cdot C_{p_{air}} \cdot \frac{dT_{ac}}{dt} = h_{pvac} (T_{ipv} - T_{ac}) + h_{wac} (T_{ac} - T_{ew}) \tag{4}$$

$$h_r (T_{ipv}^4 - T_{ew}^4) - h_{wac} (T_{ac} - T_{ew}) - \frac{(T_{ew} - T_{mw})}{\frac{R_w}{2}} = 0 \tag{5}$$

4.1.3. Heat transfer across the wall

The energy balance for the PCM wall can be obtained from Eqs. (6) and (7) where h_i is the interior heat transfer coefficient based on the Santos et al. [52] and q_i is based on the Athienitis [53] approach for



Fig. 2. Building Added PV system.



Fig. 3. Building Integrated PV system.

PCM model: (Fig. 5).

$$M_w \cdot C_{p_w} \cdot \frac{dT_{mw}}{dt} = \frac{(T_{cw} - T_{mw})}{\frac{R_w}{2}} - \frac{(T_{mw} - T_{iw})}{\frac{R_w}{2}} + q_i \quad (6)$$

$$\frac{(T_{mw} - T_{iw})}{\frac{R_w}{2}} - h_i(T_{iw} - T_{in}) = 0 \quad (7)$$

4.2. BIPVT air collector

Fig shows an elemental area $b \cdot dx$ of the BIPVT system over which solar intensity is received. The energy balance for PV module of the BIPVT system for elemental area $b \cdot dx$ is given by [54,55].

[Rate of heat received by the solar cell]+[Rate of heat received by the non-packing area]=[Rate of heat loss from PV module to air as the top loss]+[Rate of heat loss from PV module to the back surface/tedlar]+[Rate of electricity production]

$$\tau_g[\alpha_c \beta_c + (1 - \beta_c)\alpha_r]I(t)bdx = [U_T(T_c - T_a) + h_T(T_c - T_{bs})]bdx + \eta_{ca}I(t)bdx \quad (8)$$

The solar collector temperature can be obtained by simplifying Eq. (8):

$$T_c = \frac{h_T T_{bs} + U_T T_a + I(t)(\alpha\tau)_{eff}}{U_T + h_T} \quad (9)$$

For elemental area $b \cdot dx$ the energy balance of the back surface of the PV module (tedlar) is given by

[Rate of heat gain from PV module to the tedlar]=[Rate of heat loss from tedlar to air side in the duct]

$$h_T(T_c - T_{bs})bdx = h_{air}(T_{bs} - T_{air})bdx \quad (10)$$

Substituting T_c from Eq. (9) in Eq. (10), the surface temperature of the back side of PV module is obtained as:

$$T_{bs} = \frac{h_{air}T_{air} + U_T T_a + h_p I(t)(\alpha\tau)_{eff}}{U_T + h_{air}} \quad (11)$$

Energy balance for air flowing in the duct of the BIPVT system for elemental area $b \cdot dx$ is given by

[Rate of heat received from tedlar to air side in the duct]=[Rate of heat gain by air flowing in the duct of the BIPVT system]+[Rate heat loss from air through insulation]

$$h_{air}(T_{bs} - T_{air})bdx = \dot{m}_{air}C_{air} \left(\frac{dT_{air}}{dx} \right) dx + U_{bb}(T_{air} - T_r)bdx \quad (12)$$

Substituting T_{bs} from Eq. (11) in Eq. (12) we have

$$h_{air} \left[\frac{h_{p1}I(t)(\alpha\tau)_{eff} - U_{T1}(T_{air} - T_a)}{U_{T1} + h_{air}} \right] bdx = \dot{m}_{air}C_{air} \left(\frac{dT_{air}}{dx} \right) dx + U_{bb}(T_{air} - T_r)bdx$$

OR

$$\left(\frac{dT_{air}}{dx} \right) + \frac{bU_L}{\dot{m}_{air}C_{air}} T_{air} = \frac{b}{\dot{m}_{air}C_{air}} [U_{bb}T_r + U_{Tair}T_a + h_{p2}h_{p1}I(t)(\alpha\tau)_{eff}] \quad (13)$$

Integrating Eq. (13) with boundary condition at $x=0$, $T_{air} = T_r$; at $x=L$, $T_{air} = T_{airout}$ the outlet air temperature (T_{airout}) of the flowing air in the duct of the BIPVT system for length L , is given by

$$T_{airout} = \left[\frac{U_{bb}T_r + U_{Tair}T_a + h_{p2}h_{p1}I(t)(\alpha\tau)_{eff}}{U_L} \right] \left(1 - e^{-\frac{bU_L}{\dot{m}_{air}C_{air}}L} \right) + T_r e^{-\frac{bU_L}{\dot{m}_{air}C_{air}}L} \quad (14)$$

The average air temperature of the air flowing in the duct of the BIPVT system is given by

$$\bar{T}_{air} = \left[\frac{U_{bb}T_r + U_{Tair}T_a + h_{p2}h_{p1}I(t)(\alpha\tau)_{eff}}{U_L} \right] \left(1 - \frac{1 - e^{-\frac{bU_L}{\dot{m}_{air}C_{air}}L}}{\frac{bU_L}{\dot{m}_{air}C_{air}}L} \right) + T_r \frac{1 - e^{-\frac{bU_L}{\dot{m}_{air}C_{air}}L}}{\frac{bU_L}{\dot{m}_{air}C_{air}}L} \quad (15)$$

The rate of useful thermal energy obtained for η_{pv} row of the BIPVT systems is given by [66]

$$\dot{Q}_u = \eta_{pv} \times \dot{m}_{air}C_{air}(T_{airout} - T_r) = \eta_{pv} \times \dot{m}_{air}C_{air} \left[\frac{U_{bb}T_r + U_{Tair}T_a + h_{p2}h_{p1}I(t)(\alpha\tau)_{eff}}{U_L} - T_r \right] \times \left(1 - e^{-\frac{bU_L}{\dot{m}_{air}C_{air}}L} \right) \quad (16)$$

4.2.1. Room temperature

The useful thermal energy from the BIPVT system is partially used for space heating and the remaining is lost. The energy balance for the space heating of the building is given by

$$\eta_{pv} \times \dot{m}_{air}C_{air} \left[\frac{U_{bb}T_r + U_{Tair}T_a + h_{p2}h_{p1}I(t)(\alpha\tau)_{eff}}{U_L} - T_r \right] \times \left(1 - e^{-\frac{bU_L}{\dot{m}_{air}C_{air}}L} \right) + U_{bb}(\bar{T}_{air} - T_r)A_{roof} = \left(\dot{m}_r C_{air} \frac{dT_r}{dt} \right) + (UA)_t(T_r - T_a) + 0.33N_0V(T_r - T_a) \quad (17)$$





On solving Eq. (17) we have

$$\left(\frac{dT_r}{dt} \right) + \frac{1}{\dot{m}_r C_{air}} \left[(UA)_t + 0.33N_0V \right] T_r = \left\{ \eta_{pv} \times \dot{m}_{air}C_{air} \left(\frac{U_{bb}}{U_L} - 1 \left(1 - e^{-\frac{bU_L}{\dot{m}_{air}C_{air}}L} \right) \right) - U_{bb} \left(\frac{U_{bb}}{U_L} \left(1 - \frac{1 - e^{-\frac{bU_L}{\dot{m}_{air}C_{air}}L}}{\frac{bU_L}{\dot{m}_{air}C_{air}}L} \right) + \frac{1 - e^{-\frac{bU_L}{\dot{m}_{air}C_{air}}L}}{\frac{bU_L}{\dot{m}_{air}C_{air}}L} - 1 \right) A_{roof} \right\} T_r + U_{bb} \left[\frac{U_{Tair}T_a + h_{p2}h_{p1}I(t)(\alpha\tau)_{eff}}{U_L} \right] \left(1 - \frac{1 - e^{-\frac{bU_L}{\dot{m}_{air}C_{air}}L}}{\frac{bU_L}{\dot{m}_{air}C_{air}}L} \right) A_{roof} \quad (18)$$

The equation for room air temperature is obtained by applying initial condition $t=0$, $T_r = T_{ri}$ and by integrating Eq. (18).


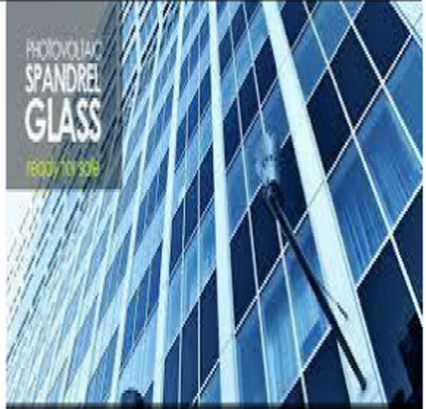

$$T_r = \frac{f(t)}{a} (1 - e^{-at}) + T_{ri} e^{-at} \quad (19)$$

Table 2
Different types of integration of PV in buildings [21].

BIPV INTEGRATION	TYPES	FEATURES	DESIGNS
Roofing System	Tiles	BIPV solar tile is a solar roofing product designed to integrate with flat concrete roof tiles.	
	Shingles	Solar Shingles or roofing systems are integrated into the roof and are therefore more visually integrated with the building than Solar Panels which are mounted on a roof or ground. Solar Shingles will protect the roof from weather like regular roof shingles.	
	Skylights	Skylight structures provide both light and electricity to the building. It is the most special application used in building similar to semitransparent facades.	
	Standing Seam Products	BIPV metal roof products converts sun’s energy to electricity 15 to 20 times more than the conventional PV panels. It can generate power in cloudy conditions as well.	

(continued on next page)

Table 2 (continued)

Facades	Curtain wall products	Solar curtain walls provides clean energy, natural illumination and thermal comfort by filtering of UV and Infra red radiation.	
	Spandrel panels	Spandrel glass panels are based on crystalline and thin film technologies. These are used in the building envelope to hide the structure or construction material.	
	Glazing	Various shapes of PV modules can be used as a shading element for windows. It also uses one way tracking mechanism for optimum orientation of PV array.	

where

$$a = \frac{1}{\dot{m}_r C_{air}} \left[\{ (UA)_t + 0.33N_0 V \} - \left\{ \eta_{pv} \times \dot{m}_{air} C_{air} \left(\frac{U_{bb}}{U_L} - 1 \left(1 - e^{-\frac{bU_L}{\dot{m}_{air} C_{air}} L} \right) \right) \right. \right. \\ \left. \left. - U_{bb} \left\{ \frac{U_{bb}}{U_L} \left(1 - \frac{1 - e^{-\frac{bU_L}{\dot{m}_{air} C_{air}} L}}{\frac{bU_L}{\dot{m}_{air} C_{air}} L} \right) + \frac{1 - e^{-\frac{bU_L}{\dot{m}_{air} C_{air}} L}}{\frac{bU_L}{\dot{m}_{air} C_{air}} L} - 1 \right\} A_{roof} \right] \right.$$

$$f(t) = \frac{1}{\dot{m}_r C_{air}} \left[\left\{ (UA)_t + 0.33N_0 V \right\} T_a \left\{ \eta_{pv} \dot{m}_{air} C_{air} \left[\frac{U_{tair} T_a + h_p 2 h_{p1} I(t) (\alpha \tau)_{eff}}{U_L} \right] \left(1 - e^{-\frac{bU_L}{\dot{m}_{air} C_{air}} L} \right) \right. \right. \\ \left. \left. + U_{bb} \left\{ \frac{U_{tair} T_a + h_p 2 h_{p1} I(t) (\alpha \tau)_{eff}}{U_L} \right\} \left(1 - \frac{1 - e^{-\frac{bU_L}{\dot{m}_{air} C_{air}} L}}{\frac{bU_L}{\dot{m}_{air} C_{air}} L} \right) \right\} A_{roof} \right] \quad [8]$$

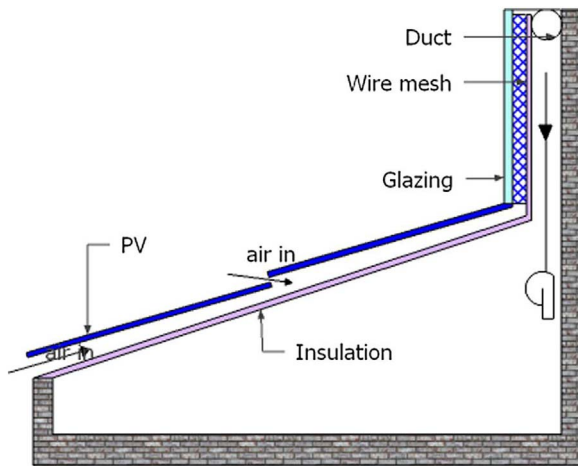


Fig. 4. BIPVT system [24].

4.3. BIPVT water collector

For the analysis, a Flat plate solar thermal collector is considered. Applying one dimensional steady state thermal model, following relations are obtained [56].

The useful heat gain of the collector is as follows

$$Q = AF_R [(\tau\alpha)_{PV}G - U_{loss}(T_1 - T_a)] \tag{20}$$

Using the mass flow rate (m) and specific heat of the collector, Heat removal factor (F_R) can be determined from the Eq. (21)

$$F_R = \frac{mC_p}{AU_{loss}} \left[1 - e^{-\frac{AU_{loss}F'}{mC_p}} \right] \tag{21}$$

The fin efficiency is calculated by using Eq. (22)

$$F = \frac{\tanh\left(M\frac{W-d}{2}\right)}{\left(M\frac{W-d}{2}\right)} \tag{22}$$

M is a factor which takes into consideration the thermal conductivity of PV cell and the absorber

$$M = \sqrt{\frac{U_{loss}}{K_{abs}L_{abs} + K_{PV}L_{PV}}} \tag{23}$$

Table 3
Different types of integration of PVT in buildings [22, 23, and 24].

BIPVT INTEGRATION	FEATURES	DESIGNS
Phase Change Materials (PCM) integrates the BIPV	Phase change material can be integrated into the BIPVT system as a thermal storage element.	
Duct design of BIPVT	Under the panel a duct has been made for the flow of air as thermal cooling medium.	
PVT Water collector integrate into the roof	A building heating system is integrated with a water type PVT collector mounted into the roof of an experimental unit	

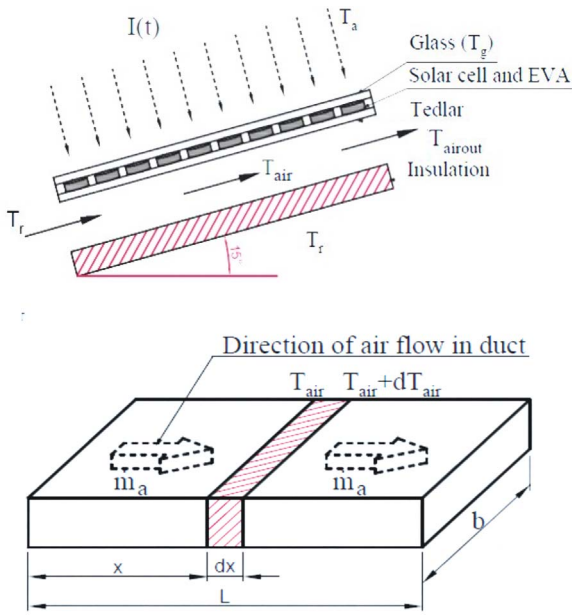


Fig. 5. Cross section of BIPVT system and an elementary area b.dx shows flow pattern of air.

Eq. (24) is used to calculate the corrected fin efficiency (F')

$$F' = \frac{\frac{1}{U_{loss}}}{W \left[\frac{1}{U_{loss}(d + (W - d)F)} \right] + \frac{1}{Wh_{pVA}} + \frac{1}{\pi dh_{fluid}}} \quad (24)$$

The overall heat loss coefficient is the summation of heat loss from the collector edge and surface losses (top & rear) [57,58]

$$U_{edge} = \frac{k_{edge}pt}{L_{edge}A_{collector}} \quad (25)$$

$$U_{top} = \left\{ \frac{N}{\frac{C}{T_{pm}} \left(\frac{T_{pm} - T_a}{N - f} \right)^e + \frac{1}{h_w}} \right\}^{-1} + \frac{\sigma(T_{pm} + T_a)(T_{pm}^2 + T_a^2)}{(\epsilon_p + 0.000591Nh_w)^{-1} + \frac{2N + f - 1 + 0.133\epsilon_p}{\epsilon_g} - N} \quad (26)$$

Where p is the collector perimeter, t is the absorber thickness

$$C = (520 - 0.000051 \beta^2)$$

$$F = (1 + 0.089 h_w - 0.116 h_w \epsilon_p) (1 + 0.07866N)$$

$$e = 0.430 \left(1 - \frac{100}{T_{pm}} \right)$$

ϵ_g the emittance of the cover or glazing, ϵ_p the emittance of the plate, β is the collector mounting, σ is the Stefan-Boltzmann constant, N is the number of covers or glazing layers, and h_w is the convective heat transfer coefficient due to the wind.

$$T_{pm} = T_r + \frac{Q}{F_R U_{loss}} (1 - F_R) \quad (27)$$

Eq. (28) is used to determine the radiation heat transfer coefficient as a function of sky temperature (T_s), the mean collector plate temperature (T_{pm}) and the plate emissivity (ϵ_p) [59]

$$h_r = \sigma \epsilon_p (T_{pm}^2 + T_s^2) (T_{pm} + T_s) \quad (28)$$

Modified sky temperature [59] is represented by Eq. (29) as a function of the ambient temperature

$$T_s = 0.037536T_a^{1.5} + 0.32T_a \quad (29)$$

The forced convection heat transfer coefficient (h_w) is calculated using wind velocity (v)

$$h_w = 2.8 + 3.0v \quad (30)$$

Natural convection heat transfer coefficient (h_{nat}) is a function of the temperature difference between the mean collector plate temperature (T_{pm}) and the ambient temperature (T_a) [59]

$$h_{nat} = 1.78(T_{pm} - T_a)^{1/3} \quad (31)$$

The overall top loss heat transfer coefficient (U_{top}) is the summation of the convection and radiation losses

$$h_c = \sqrt{h_w^3 + h_{nat}^3} \quad (32)$$

The heat loss from the rear surface of the BIPVT can be calculated using Eq. (33) [60]

$$Nu = 0.286A^{-0.286}Gr^{1/4} \quad (33)$$

The Grashof number is determined based on the properties at average ambient temperature and BIPVT mean temperature.

$$Gr = \frac{g\beta(T_{pm} - T_a)H^3}{\nu^2} \quad (34)$$

Grashof number is used to determine natural convection heat transfer coefficient and the Overall heat transfer coefficient

$$Q = S[AF_R[\tau\alpha_{pV} \cdot G - U_{loss}(T_1 - T_2)]] \times (1 - S)[AF_R[\tau\alpha_T \cdot G - U_{loss}(T_1 - T_2)]] \quad (35)$$

The thermal performance of the BIPVT collector can be determined by modifying Eq. (20) with the inclusion of packing factor (S) and the product of transmittance-absorptance of the collector material ($\tau\alpha_T$) on to which the PV cells are laminated, as shown in Eq. (35).

The useful heat gain by the solar collector and the mean temperature of the BIPVT (T_{pm}) can be calculated from Eq. (35).

The electrical efficiency can be calculated based on the temperature difference (mean temperature of the BIPVT minus Nominal Operating Cell Temperature (NOCT)) with the following assumptions. (NOCT=298 K, Standard efficiency of solar cell=15%, Temperature coefficient=0.5%/°C [61])

$$\eta_{electrical} = 0.15(1 - 0.005(T_{pm} - NOCT)) \quad (36)$$

Finally the thermal efficiency equation of the BIPVT is developed from the transmittance-absorptance product and the packing factor

$$\eta_{thermal} = F_R((S \times \tau\alpha_{pV}) + (1 - S) \times \tau\alpha_T) - F_R U_{loss} \times \frac{T_r - T_a}{G} \quad (37)$$

5. Energy and exergy analysis of BIPV and BIPVT

5.1. Exergy analysis of BIPV system

The exergy efficiency of a system is given as

$$\Psi = \frac{\dot{E}_x}{E_{x,solar}} \quad (38)$$

where \dot{E}_x the exergy of the BIPV system is mainly electrical power output of the system [62–64]

$$\text{And } \dot{E}_x = V_m I_m \left[1 - \left(\frac{T_{amb}}{T_{mod}} \right) \right] \dot{Q} \quad (39)$$

where \dot{Q} is the convective and radiative heat transfer coefficient from photovoltaic cell to ambient and

$$\dot{Q} = h_{ca}A_{mod}(T_{mod} - T_{amb}) \tag{40}$$

where $h_{ca} = 5.7 + 3.8V_w$ (41)

V_w = wind velocity.

$$\text{Then } \dot{E}_x = VmIm - \left[1 - \left(\frac{T_{amb}}{T_{mod}} \right) \right] [h_{ca}A_{mod}(T_{mod} - T_{amb})]$$

and $\dot{E}_{x_{solar}}$ is the exergy rate from the solar irradiance in W/m^2 is given as [62,63]

$$\dot{E}_{x_{solar}} = \left[1 - \left(\frac{T_{amb}}{T_{mod}} \right) \right] I_s A_{mod} \tag{42}$$

Then exergy efficiency of the BIPV system can be given as [63]

$$\Psi_{PV} = \frac{V_m I_m - \left[1 - \left(\frac{T_{amb}}{T_{mod}} \right) \right] (5.7 + 3.8 V_w)}{\left[1 - \left(\frac{T_{amb}}{T_{mod}} \right) \right] (I_s A_{mod})} \tag{43}$$

The exergy rate of solar irradiance can also be calculated by using Petela's formula [63,64]

$$\Psi_{PV} = \frac{V_m I_m - \left[1 - \left(\frac{T_{amb}}{T_{mod}} \right) \right] [h_{ca}A_{mod}(T_{mod} - T_{amb})]}{\left[1 + \left(\frac{1}{3} \right) \left(\frac{T_{amb}}{T_{sun}} \right)^4 - \left(\frac{4}{3} \right) \left(\frac{T_{amb}}{T_{sun}} \right) \right] (I_s A_{mod})} \tag{44}$$

5.2. Energy analysis of BIPVT system

Energy analysis is based on the first law of thermodynamics.

Thermal Efficiency:

$$\eta_{TH} = \frac{\text{Net Thermal Output}}{\text{Net Solar Insolation}} = \frac{\sum_{i=1}^T \dot{Q}_u}{\sum_{i=1}^T I(t)bL} \tag{45}$$

Electrical Efficiency:

$$\eta_E = \frac{\sum_{i=1}^T \eta_{ca} I(t)bL}{\sum_{i=1}^T I(t)bL} \tag{46}$$

Total efficiency or PVT efficiency:

It is used to evaluate the overall performance of the system [62–64]

$$\eta_{PVT} = \eta_{TH} + \eta_{PV} \tag{47}$$

Primary energy saving efficiency.

It is proposed as a performance indicator to recognize the energy

Table 4
Features of BIPV and BIPVT System design software.

Name of the software	Features
SOLCEL-II	i) In order to predict PV output ambient temperature, wind speed, hourly values of the horizontal and direct normal radiation and in-plane insolation are used [25]. ii) The hourly performance of the system can be simulated by employing floating battery; maximum power tracking; temperature degraded efficiency and voltage regulator. iii) Energy analysis and performance simulation of BIPV system can be carried out [25].
PV FORM	i) It can perform simulation of grid connected and stand-alone system. The input data required for simulation are: Ambient temperature, global horizontal insolation, and wind speed [25].
TRNSYS	i) Maximum power point tracking and part load efficiency of power conditioning unit can also be considered [27]. ii) Algebraic differential equations are used to describe the analytical or empirical component models [26]. iii) Individual components are interconnected to perform system simulation [27]. iv) Energetic simulation can be carried [27].
CFD, ANSYS fluent	i) Energetic and thermal simulation of BIPVT is done. ii) Energetic simulation of BI solar thermal system, BI solar chimney can be done. iii) Thermal simulation of BI skin facades, BI Trombe wall and several systems can be done. iv) Optical simulation of BI several systems is done [28–39].
COMSOL Multiphysics	Thermal simulation of BI skin facades is done using this software [40].
RADIANCE	Optical simulation of several BI systems can be done [41].
MATLAB	i) Thermal simulation of BI pipes can be done. ii) Thermal and energetic simulation of BI solar thermal is also possible.
PV f-Chart	iii) Energetic and thermal simulation of BIPVT can be done [42–47]. i) PV systems design and analysis can be carried out [12]. ii) Module temperature is used to calculate the array efficiency calculated [46].
PVSYST	iii) The total in plane solar radiation on the horizontal surface is used to calculate the performance of the PV system. iv) Daily, monthly and annual average performance of PV system can be predicted from the weather data [47].
PVSOL	i) It is used for design and performance analysis of grid-connected and stand-alone and PV systems [12]. ii) Inbuilt geographical and meteorological data is used for simulation [46,47]. iii) 3D visualization and shading effect is possible [46,47]. iv) Following losses are considered including temperature losses, mismatch losses, and reflection losses [46,47]. v) Inverter(s) configurations and load profiles can be varied and modeled [46,47].
PVSOL	i) PV systems can be designed, optimized [12]. ii) The software has inbuilt PV module and inverter database [46,47]. iii) It can perform simulation by constraining the following factors: varying orientation, shading effect, partial load characteristics of inverter, inverter sizing, and varying load profile [46,47].
PVWATTS	iv) Economic analysis can be performed for various utility tariff rates [46,47].
ENERGY-10 PV	It is an internet based online tool to simulate the energy generation of grid connected photovoltaic system applicable for US location [46,47]. i) ENERGY-10 tool uses TRNSYS program to determine the performance of photovoltaic system [46,47].
PVSMI	ii) It can also be used to study the hourly interaction between the PV array and building load of grid connected BIPV system [12]. i) Modeling and study of VI characteristics of PV cell, module and array [46].
PHANTASM	ii) Effect of bypass diodes and blocking diode can be studied [47]. i) It is an extension of TRNSYS software developed to study the Building Integrated Photovoltaic applications [12,46,47]. ii) It uses various subroutines for performance simulation [12,46,47]. iii) Electrical parameters, NOCT, electron band gap, absorptance of PV cell, transmittance of the glazing are required for simulation.

Table 5
Comparative studies of BIPV AND BIPVT at different location [70–81].

BIPV	Location	Efficiency	Features	BIPVT	Location	Efficiency	Features
	Italy	The highest value of Ross coefficient (k) i.e. highest module temperature at a certain G is found for three glass to glass module types. The glass-tedlar module types operate at slight lower temperature.	Overview of value of k for different module types according to monitored data registered over one year time period is carried out.		South Korea	Average thermal and electrical efficiency is 30% and electrical efficiency is 17%.	Heating system combined with a water-type PVT collector integrated into the roof of an experimental unit is analyzed
	Cyprus	With an air gap of 0.02 m between the building and PV panel and air velocity of 0.5 m/sec the mean temperature of the panel is decreased from 77 °C to 39 °C which in turn increases the efficiency. For a steady velocity of 0.2 m/sec temperature of the building varies from 23.7 °C for a width of 0.01–20 °C for a width of 0.05 m	Effect of air flow in a BIPV panel is examined.		India	HIT produces maximum annual electrical energy (810 kW h) and Si produces maximum annual thermal energy (464 kW h) Annual overall thermal energy (2497 kW h) and exergy (834 kW h) is maximum for HIT PV module	Building Integrated semitransparent photovoltaic thermal (BISPVT) system integrated to the roof of a room.
	Hongkong	Annual thermal efficiency is found 37.5% and electrical efficiency is 9.39%.	BIPVT water heating system is installed on vertical wall of a fully air conditioned building. The system is equipped with PV cells and flat plate thermal absorber.		Malaysia	Primary energy saving efficiency produced from a BIPVT system is about 73–81%. PVT energy efficiency of 55–62% is higher than the PVT exergy efficiency of 12–14% in an hourly variation of a BIPVT system.	A high efficiency multycrystal photovoltaic (PV) module and spiral flow absorber has been designed, performed and investigated.
	India	The detailed analysis of the model indicates that performance and life enhancement of BIPV module could be achieved with 10 °C cooling without loss of power.	The dynamic model of BIPV/Thermoelectric system considering the PV panel temperature has been developed.		Canada	Thermal efficiency of the BIPVT system is increased by 5–8% and marginal increase in electrical efficiency. Addition of wire mesh packing in the collector improved the thermal efficiency by 10%.	A BIPVT model is integrated into a existing solar house. The system is analyzed for multiple inlets and effect of glazing.
	Korea	Energy generation Efficiency is enhanced up to 47% by varying the location of building in terms of azimuth and reducing the shading.	BIPV thin film amorphous modules are integrated into the windows and façade of the building.		China	BIPVT is applied to the ETFE cushion structure and its technical feasibility is evaluated.	Experimental set up consisting of ETFE cushion structure has been designed and developed. Experiments are carried out for various climatic conditions.
	Germany	Maximum electrical efficiency reach up to 10% and the thermal one is 12%.	Modeling of hybrid BIPV-PCM is done		India	Annual electrical exergy is 16,209 kW h and thermal exergy is 1531 kW h with overall thermal efficiency is 53.7%	BIPVT is installed on the rooftop of a building (area=65 m ²). This analysis is carried out to identify the best design for application in cold climates.
	Turkey	Daily average electrical efficiency is 4.52% and thermal efficiency is 27.2%	a-Si semi transparent PV module is integrated on Trombe wall façade		India	The electrical efficiency of the system and room temperature (without air duct) is found to be 7.25% and 18.7 °C respectively, whereas with air duct it is found to be 7.57% and 15.2 °C respectively.	Thin Film based PV Modules is used in the Building integrated opaque photovoltaic thermal (BIOOPT) systems.

grade difference between thermal and electrical energy. This indicator is often used because as it addresses both the quality and quantity of the energy that PVT system converts.

[62–64]

$$\eta_f = \frac{\eta_{PV}}{\eta_p} + \eta_{th} \quad (48)$$

5.3. Exergy analysis of BIPVT system [70]

Exergy analysis is based on the second of law of thermodynamics, which if the effects due to the kinetic and potential energy changes are neglected, the general exergy balance can be expressed in rate form as given [65,66]

$$\sum Ex_{in} - \sum Ex_o = \sum Ex_d \quad (49)$$

$$\sum Ex_{in} - \sum (Ex_{th} + Ex_{PV}) = \sum Ex_d \quad (50)$$

where,

$$Ex_{in} = A_c N_c S \left[1 - \frac{4}{3} \left(\frac{T_a}{T_s} + \frac{1}{3} \left(\frac{T_a}{T_s} \right)^4 \right) \right] \quad (51)$$

$$Ex_{th} = Q_u \left(1 - \frac{T_a + 273}{T_o + 273} \right) \quad (52)$$

$$Ex_{PV} = \eta_c A_c N_c S \left[1 - \frac{4}{3} \left(\frac{T_a}{T_s} + \frac{1}{3} \left(\frac{T_a}{T_s} \right)^4 \right) \right] \quad (53)$$

$$Ex_{PVT} = Ex_{th} + Ex_{PV} \quad (54)$$

where Ex_{in} is input exergy (radiation exergy), Ex_o is output exergy, Ex_{th} is thermal exergy, Ex_{PVT} is photovoltaic thermal exergy, A_c is collector area, N_c is number of collectors, S is solar radiation, T_a is ambient temperature and T_s is sun temperature ($T_s=5777$ K). The exergy destruction (Ex_d) or irreversibility may be expressed as [67,68]

$$Ex_d = T_a S_{gen} \quad (55)$$

where S_{gen} is entropy generation rate. While the irreversibility of any energy process is at minimum, the improvement in the exergy efficiency is at maximum. The concept of an exergetic “improvement potential” (IP) could be considered as a very useful tool to analyzing systems or process more efficiently. The IP of a system or process is given by: [68,69]

$$IP = (1 - \eta_{ex}) \dot{Ex}_d \quad (56)$$

where η_{ex} is the second law efficiency may be expressed as (Table 5).

$$\eta_{ex} = 1 - \frac{Ex_d}{Ex_{in}} \quad (57)$$

6. Performance comparison of BIPV and BIPVT

See Table 4.

7. Conclusion

The motivation of this review is to analyze the thermal performance of BIPV and BIPVT system according to the various modeling techniques and simulation software. After rigorous literature review on BIPV & BIPVT system the following key conclusions are drawn.

1. The operating temperature of both BIPV and BIPVT systems plays an important role in the efficiency and thermal performance.
2. BIPV and BIPVT systems are capable of fulfilling the partial/complete energy requirements of the building.
3. BIPV-T is very attractive and more preferable than BIPV as they produce both thermal and electrical energy using the same roof or

facade area.

4. The thermal energy of BIPV-T can be converted into useful affordable energy. The economic -benefit of BIPV can be increased by utilizing the thermal energy.
5. Continuous innovations in both BIPVT and BIPV technologies will yield better cost solutions and improved building integration solutions.

References

- [1] Makki Adham, Omer Siddig, Sabir Hisham. Advancements in hybrid photovoltaic systems for enhanced solar cells performance. *Renew Sustain Energy Rev* 2015;41:658–84.
- [2] Buonomano Annamaria, Calise Francesco, Palombo Adolfo, Vicidomini Maria. BIPVT systems for residential applications: an energy and economic analysis for European climates. *Appl Energy* 2016, [xxx–xxx].
- [3] Rajoria CS, Agrawal Sanjay, Subhash Chandr , Tiwari GN, Chauhan DS, Novel A. investigation of building integrated photovoltaic thermal (BIPVT) system: a comparative study. *Sol Energy* 2016;131:107–18.
- [4] Shan F, Tang F, Cao L, Fang G. Performance evaluations and applications of photovoltaic–thermal collectors and systems. *Renew Sustain Energy Rev* 2014;33:467–83.
- [5] Pandey AK, Tyagi VV, JeyrajA/LSelvaraj , Rahim NA, Tyagi SK. Recent advances in solar photovoltaic systems for emerging trends and advanced applications. *Renew Sustain Energy Rev* 2016;53:859–84.
- [6] Leone Giuliana, Beccali Marco. Use of finite element models for estimating thermal performance of façade-integrated solar thermal collectors. *Appl Energy* 2016;171:392–404.
- [7] Chen Fangliang, Yin Huiming. Fabrication and laboratory-based performance testing of a building-integrated photovoltaic-thermal roofing panel. *Appl Energy* 2016;177:271–84.
- [8] Agrawal Basant, Tiwari GN. Optimizing the energy and exergy of building integrated photovoltaic thermal (BIPVT) systems under cold climatic conditions. *Appl Energy* 2010;87:417–26.
- [9] Wronski CR, Von Roedern B, Ko"odziej A. Thin-film Si: h-based solar cells. *Vacuum* 2008;82:1145–50.
- [10] Tiwari GN, Mishra RK, Solanki SC. Photovoltaic modules and their applications: a review on thermal modeling. *Appl Energy* 2011;88:2287–304.
- [11] Chow TT. A review on photovoltaic/thermal hybrid solar technology. *Appl Energy* 2010;87:365–79.
- [12] Lamnatou Chr, Mondol JD, Chemisana D, Maurer C. Modelling and simulation of building-integrated solar thermal systems: behaviour of the system. *Renew Sustain Energy Rev* 2015;45:36–51.
- [13] Prof KL Chopra Former Director, IIT Kharagpur Founder, Thin Film Laboratory, IIT Delhi & Microscience Laboratory, IIT Kharagpur. *Thin Film Solar Cells (A Status Review)*.
- [14] Seth Pooja, Aggarwal Shruti, Sharma Avinash C, Rao SM, Verma RC. Growth of lithium fluoride crystals by edge defined film fed growth [June]. *Indian J Pure Appl Phys* 2010;48:394–7.
- [15] R  ther R, Beyer HG, Montenegro AA, Dacoregio MM, Salamoni IT, Knob P. Performance results of the first grid connected thin film PV installation in Brazil: high performance ratios over 6 years of continuous operation. In: *Proceedings of the 19th European photovoltaic solar energy conference, Paris, France. p. 1487–90; 2004.*
- [16] Yamawaki T, Mizukami S, Masui T, Takahashi H. Experimental investigation on generated power of amorphous PV module for roof azimuth. *Sol Energy Mater Sol Cells* 2001;67:369–77.
- [17] Nann S, Emery K. Spectral effects on PV-device rating. *Sol Energy Mater Sol Cells* 1992;27:189–216.
- [18] SANYO, Sanyo Solar Ark, (<http://www.sanyo.com/industrial/solar>).
- [19] Vats Kanchan, Tiwari GN. Energy and exergy analysis of a building integrated semitransparent photovoltaic thermal (BISPVT) system. *Appl Energy* 2012;96:409–16.
- [20] Delisle V  ronique, Kummert Micha  l. Cost-benefit analysis of integrating BIPV-T air systems into energy-efficient homes. *Sol Energy* 2016;136:385–400.
- [21] Peng Changhai, Huang Ying, Wu Zhishen. Building-integrated photovoltaics (BIPV) in architectural design in China. *Energy Build* 2011;43:3592–8.
- [22] Kim Jin-Hee, Park Se-Hyeon, Kang Jun-Gu, Kim Jun-Tae. Experimental performance of heating system with building integrated PVT (BIPVT) collector. *Energy Procedia* 2014;48:1374–84.
- [23] Tiwari ProfGN. Centre for Energy Studies Indian Institute of Technology (IIT) Delhi & BAG Energy Research Society (BERS). Performance evaluation of bipvt systems.
- [24] Yang Tingting, Andreas K. Athienitis. A study of design options for a building integrated photovoltaic/thermal (BIPV/T) system with glazed air collector and multiple inlets. *Sol Energy* 2014;104:82–92.
- [25] Yoo SH. Simulation for an optimal application of BIPV through parameter variation. *Sol Energy* 2011;85:1291–301.
- [26] Davidsson H, Perers B, Karlsson B. Performance of a multifunctional PV/T hybrid solar window. *Sol Energy* 2010;84:365–72.
- [27] Mondol JD, Yohanis YG, Smyth M, Norton B. Long-term validated simulation of a building integrated photovoltaic system. *Sol Energy* 2005;78:163–76.
- [28] Windholz B, Zauner C, Rennhofer M, Schranzhofer H. Solar thermal energy

- conversion and photovoltaics in a multifunctional facade. In: Proceedings of the CISBAT. Lausanne, Switzerland, 14–16 September; 2011.
- [29] DeBlois JC, Bilec MM, Schaefer LL. Design and zonal building energy modeling of a roof integrated solar chimney. *Renew Energy* 2013;52:241–50.
- [30] Coussirat M, Guardo A, Jou E, Egusquiza E, Cuerva E, Alavedra P. Performance and influence of numerical sub-models on the CFD simulation of free and forced convection in double glazed ventilated façades. *Energy Build* 2008;40:1781–9.
- [31] Pérez-Grande I, Meseguer J, Alonso G. Influence of glass properties on the performance of double-glazed facades. *Appl Therm Eng* 2005;25:3163–75.
- [32] Nassim Safer N, Woloszyn M, Roux JJ. Three-dimensional simulation with a CFD tool of the air flow phenomena in single floor double-skin façade equipped with a Venetian blind. *SolEnergy* 2005;79:193–203.
- [33] Pasut W, DeCarli M. Evaluation of various CFD modeling strategies in predicting air flow and temperature in a naturally ventilated double skin facade. *Appl Therm Eng* 2012;37:267–74.
- [34] Jiru TE, Haghight F. Modeling ventilated double skin facade – A zonal approach. *Energy Build* 2008;40(8):1567–76.
- [35] Koyunbaba BK, Yilmaz Z, Ulgen K. An approach for energy modeling of a building integrated photovoltaic(BIPV) Trombwall system. *Energy Build* 2013;67:680–8.
- [36] Gan G. Numerical determination of adequate air gaps for building-integrated photovoltaics. *Sol Energy* 2009;83:1253–73.
- [37] Sanjuan C, Suárez MJ, González M, Pistono J, Blanco E. Energy performance of an open-joint ventilated façade compared with a conventional sealed cavity facade. *SolEnergy* 2011;85:1851–63.
- [38] Liao L, Poissant Y, Collins M, Athienitis AK, Candanedo L, Park KW. Numerical and experimental study of heat transfer in a BIPV-thermal system. *J Sol Energy Eng* 2007;129:423–30.
- [39] Li S, Karava P, Currie S, Lin WE, Savory E. Energy modeling of photovoltaic thermal systems with corrugated unglazed transpired solar collectors – part 1: model development and validation. *SolEnergy* 2014;102:282–96.
- [40] Guillén I, Gómez-Lozano V, Fran JM, López-Jiménez PA. Thermal behavior analysis of different multilayer facade: numerical model versus experimental prototype. *EnergyBuild* 2014;79:184–90.
- [41] Sprenger W. Electricity Yield Simulation of Complex BIPV Systems [Ph.D thesis]. Stuttgart: Delft University of Technology, Fraunhofer Verlag; 2013.
- [42] Notton G, Motte F, Cristofari C, Canaletti JL. New patented solar thermal concept for high building integration: test and modelling. *Energy Procedia* 2013;42:43–52.
- [43] Motte F, Notton G, Cristofari C, Canaletti JL. A building integrated solar collector: performances characterization and first stage of numerical calculation. *Renew Energy* 2013;49:1–5.
- [44] Albanese MV, Robinson BS, Brehob EG, Sharp MK. Simulated and experimental performance of a heat pipe assisted solar wall. *SolEnergy* 2012;86:1552–62.
- [45] Aelenei L, Pereira R. Innovative solutions for net zero-energy building: BIPV-PCM system – modeling, design and thermal performance. In: Proceedings of the IYCE conference. Siofok, Hungary, 6–8 June; 2013.
- [46] Kane A, Verma V. Performance enhancement of building integrated photo-voltaic module using thermoelectric cooling. *Int J Renew Energy Res* 2013;3:2.
- [47] Norton Brian, Eames Philip C, Mallick Tapas K, Huang Ming Jun, McCormack Sarah J, Mondol Jayanta D, Yohanis Yizgaw G. Enhancing the performance of building integrated photovoltaics. *Sol Energy* 2011;85:1629–64.
- [48] Test FL, Lessmann RC, Johary A. Heat transfer during wind flow over rectangular bodies in the natural environment. *J Heat Transf* 1981;103:262.
- [49] Duffie AJ, Beckman AW. *Solar Engineering of Thermal Processes*, 2nd ed.. INC: John Wiley & Sons; 1980.
- [50] Kalogirou SA. *Solar Energy Engineering - Processes and Systems*, 1st ed.. London: Elsevier; 2009.
- [51] Jaber S, Ajib S. Optimum design of Trombe wall system in mediterranean region. *Sol Energy* 2011;85:1891–8.
- [52] CAP dos Santos, Matias LMC. *Coefficientes de Transmissão Térmica De Elementos da Envolvente do Edifícios*, 1st ed. Lisboa: LNEC; 2006.
- [53] Athientis AK, Liu C, Hawes D, Banu D, Feldman D. Investigation of the thermal performance of a passive solar test-room with wall latent heat storage. *Build Environ* 1997;32:405–10.
- [54] Nayak S, Tiwari GN. Energy and exergy analysis of photovoltaic/thermal integrated with a solar greenhouse. *Energy Build* 2008;40(11):2015–21.
- [55] Tiwari A, Sodha MS. Performance evaluation of solar PV/T system: an experimental validation. *Sol Energy* 2006;80(7):751–9.
- [56] Yoo Seung-Ho, Manz Heinrich. Available remodeling simulation for a BIPV as a shading device. *Sol Energy Mater Sol Cells* 2011;95:394–7.
- [57] Vokas G, Christandonis N, Skittides F. Hybrid photovoltaic thermal systems for domestic heating and cooling-A theoretical approach. *Sol Energy* 2006;80(5):607–15.
- [58] Eicker U. *Solar Technologies for Buildings*. Chichester: John Wiley and Sons; 2003.
- [59] Fuentes MK. *A simplified Thermal Model for Flat-plate Photovoltaic Arrays*, Sandia National Laboratories Report, SAND85-0330- UC-63, Albuquerque; 1987.
- [60] Ridouane EH, Campo A. Experimental-based correlations for the characterization of free convection of air inside isosceles triangular cavities with variable apex angles. *Exp Heat Transf* 2005;18(2):81–6.
- [61] Green M. *Solar Cells: Operating Principles, Technology and System Applications*. Kensington, Australia: the University of New South Wales; 1998.
- [62] He W, Zhang Y, Ji J. Comparative experiment study on photovoltaic and thermal solar system under natural circulation of water. *Appl Therm Eng* 2011;31:3369–76.
- [63] Zhang X, Zhao X, Smith S, Xu J, Yu X. Review of R & D progress and practical application of the solar photovoltaic/thermal (PV/T) technologies. *Renew Sustain Energy Rev* 2012;16:599–617.
- [64] Radziemska E. Performance analysis of a photovoltaic-thermal integrated system. *Int J Photo Energy* 2009:1–6.
- [65] Tiwari A, Dubey S, Sundhu GS, Sodha MS, Anwar SI. Exergy analysis of integrated photovoltaic thermal solar water heater under constant flow rate and constant collection temperature modes. *Appl Energy* 2009;86:2592–7.
- [66] Mishra RK, Tiwari GN. Energy matrices analyses of hybrid photovoltaic thermal (HPVT) water collector with different PV technology. *Sol Energy* 2013;91:161–73.
- [67] Fudholi A, Sopian K, Ruslan MH, Othman MY. Performance and cost benefits analysis of double-pass solar collector with and without fins. *Energy Convers Manag* 2013;76:8–19.
- [68] Fudholi A, Sopian K, Othman MY, Ruslan MH, Bakhtyar B. Energy analysis and improvement potential of finned double-pass solar collector. *Energy Convers Manag* 2013;75:234–40.
- [69] Akpınar EK. Drying of mint leaves in solar dryer and under open sun: modeling, performance analyses. *Energy Convers Manag* 2010;51:2407–18.
- [70] Gaur Ankita, Tiwari GN. Analytical expressions for temperature dependent electrical efficiencies of thin film BIPVT systems. *Appl Energy* 2015;146:442–52.
- [71] Koyunbaba Basak Kundakci, Yilmazb Zerrin, Ulgen Koray. An approach for energy modeling of a building integrated photovoltaic (BIPV) Trombe wall system. *Energy Build* 2013;67:680–8.
- [72] Chow TT, Chan ALS, Fong KF, Lin Z, He W, Ji J. Annual performance of building-integrated photovoltaic/water-heating system for warm climate application. *Appl Energy* 2009;86:689–96.
- [73] Yoon Jong-Ho, Song Jonghwa, Lee Sung-Jin. Practical application of building integrated photovoltaic (BIPV) system using transparent amorphous silicon thin-film PV module. *Sol Energy* 2011;85:723–33.
- [74] Chow TinTaiCHAN, Lok Shun Apple FONG, Kwong Fai Square LIN, John Z, He W, Ji J. Annual performance of building-integrated photovoltaic/water-heating system for warm climate application. ELSEVIER ISSN: 0306–2619.
- [75] Ibrahim Adnan, Fudholi Ahmad, Sopian Kamaruzzaman, Othman Mohd Yusof, Ruslan Mohd Hafidz. Efficiencies and improvement potential of building integrated photovoltaic thermal (BIPVT) system. *Energy Convers Manag* 2014;77:527–34.
- [76] Hu Jianhui, Chen Wujun, Zhao Bing, Song Hao. Experimental studies on summer performance and feasibility of a BIPV/T ethylene tetrafluoroethylene (ETFE) cushion structure system. *Energy Build* 2014;69:394–406.
- [77] Ghani F, Duke M, Carson JK. Estimation of photovoltaic conversion efficiency of a building integrated photovoltaic/thermal (BIPV/T) collector array using an artificial neural network. *Sol Energy* 2012;86:3378–87.
- [78] Maturia Laura, Belluardo Giorgio, Moser David, Buono Matteo Del. BiPV system performance and efficiency drops: overview on PV module temperature conditions of different module types. *Energy Procedia* 2014;48:1311–9.
- [79] Penga Changhai, Huang Ying, Wu Zhishen. Building-integrated photovoltaics (BIPV) in architectural design in China. *Energy Build* 2011;43:3592–8.
- [80] Lamnatou Chr, Notton G, Chemisana D, Cristofari C. Life cycle analysis of a building-integrated solar thermal collector, based on embodied energy and embodied carbon methodologies. *Energy Build* 2014;84:378–87.
- [81] debarma Mary, Sudhakar K, Baredar Prashant. Comparison of BIPV and BIPVT: a review. *Resour-Effic Technol* 2016. <http://dx.doi.org/10.1016/j.reffit.2016.11.013>.